Docking and Database Screening Reveal New Classes of *Plasmodium falciparum* Dihydrofolate Reductase Inhibitors

Giulio Rastelli,*,[†] Sara Pacchioni,[†] Worachart Sirawaraporn,[‡] Rachada Sirawaraporn,[‡] Marco Daniele Parenti,[†] and Anna Maria Ferrari[†]

Dipartimento di Scienze Farmaceutiche, Università di Modena e Reggio Emilia, Via Campi 183, 41100 Modena, Italy, and Department of Biochemistry, Faculty of Science, Mahidol University, Bangkok 10400, Thailand

Plasmodium falciparum dihydrofolate reductase (PfDHFR) is an important target for antimalarial chemotherapy. Unfortunately, the emergence of resistant parasites has significantly reduced the efficiency of classical antifolate drugs such as cycloguanil and pyrimethamine. In this study, an approach toward molecular docking of the structures contained in the Available Chemicals Directory (ACD) database to search for novel inhibitors of PfDHFR is described. Instead of docking the whole ACD database, specific 3D pharmacophores were used to reduce the number of molecules in the database by excluding a priori molecules lacking essential requisites for the interaction with the enzyme and potentially unable to bind to resistant mutant PfDHFRs. The molecules in the resulting "focused" database were then evaluated with regard to their fit into the PfDHFR active site. Twelve new compounds whose structures are completely unrelated to known antifolates were identified and found to inhibit, at the micromolar level, the wild-type and resistant mutant PfDHFRs harboring A16V, S108T, A16V + S108T, C59R + S108N + I164L, and N51I + C59R + S108N + I164L mutations. Depending on the functional groups interacting with key active site residues of the enzyme, these inhibitors were classified as *N*-hydroxyamidine, hydrazine, urea, and thiourea derivatives. The structures of the complexes of the most active inhibitors, as refined by molecular mechanics and molecular dynamics, provided insight into how these inhibitors bind to the enzyme and suggested prospects for these novel derivatives as potential leads for antimalarial development.

Introduction

The dihydrofolate reductase domain of *Plasmodium falciparum* bifunctional dihydrofolate reductase−thymidylate synthase (DHFR−TS) is a validated target of antimalarial antifolates, namely, pyrimethamine (Pyr) and cycloguanil (Cyc). Alarmingly, resistance of malarial parasites to both antimalarials including their combination with sulfonamide, i.e., pyrimethamine−sulfadoxine (PS), is widespread, and therefore, there is an urgent need to search for new targets and/or new effective inhibitors to combat the resistant parasites.[1]

A wealth of information accumulated during the past decade has suggested that increasing antifolate resistance in *P. falciparum* malaria is due to accumulation of point mutations in the DHFR domain, principally at codons 16, 51, 59, 108, and 164.[2,3] In vitro experiments using synthetic genes for single and multiple mutant *Plasmodium falciparum* dihydrofolate reductase (PfDHFR) provided understanding of the role(s) of these residues and the pathway by which antifolate-resistant parasites are developed.[4] Models of PfDHFR have also been reported based on the homology of the DHFR sequences[5−7] and have been exploited to study the molecular interactions between the active site residues of the enzyme and antifolates such as Pyr, Cyc, and WR99210 (6,6-dimethyl-1-[3-(2,4,5-trichlorophenoxy)-propoxy]-1,6-dihydro-[1,3,5]triazine-2,4-diamine).[6,8] These studies highlighted the "steric constraint hypothesis" as a fundamental basis of antifolate resistance and provided rational approaches for designing inhibitors devoid of substituents at position where steric clash can likely be formed.[6,8,9]

Molecular docking and de novo design are widely applied to the discovery of enzyme inhibitors with specific and desired chemical properties.[10−13] One efficient approach for designing new inhibitors is to select, within structural databases of several thousands of known and available organic molecules, compounds that display the highest steric and electrostatic complementarity with the site of action.[14−16] In this context, docking of the 3D databases of organic molecules into the crystal structures of enzymes often provides an efficient means toward selecting small subsets of interesting and promising candidates for biological testing. The approach is straightforward, since a huge number of molecules contained in 3D databases can be rapidly screened to select for novel chemical scaffolds that are completely unrelated to known substrates or inhibitors.

In the present work, we describe a molecular docking strategy aimed at discovery of new inhibitors of PfDHFR. After prefiltering the Available Chemicals Directory (ACD) database for compounds possessing specific chemical features previously recognized to be crucial for inhibition, the focused database thus generated was docked into the 3D-homology model of the wild-type PfDHFR.[6] The study led to the identification of 12 new compounds whose chemical structures are completely

* To whom correspondence should be addressed. E-mail: rastelli.giulio@unimo.it. Phone: 0039-059-2055145. Fax: 0039-059-2055131.
  † Università di Modena e Reggio Emilia.
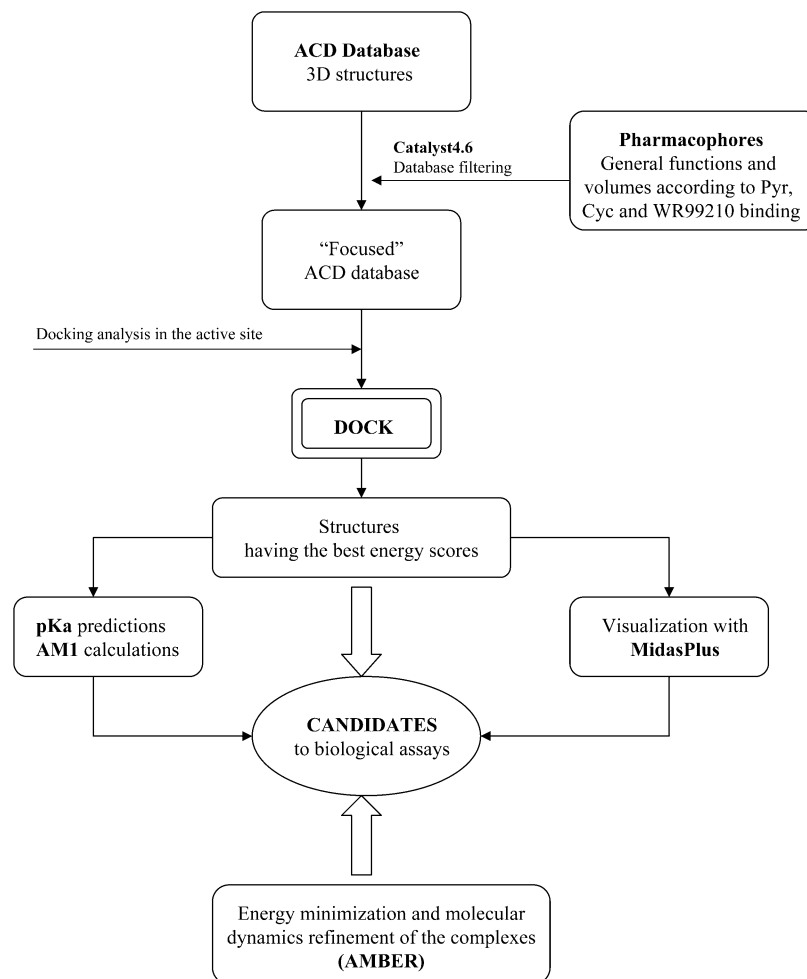 ‡ Mahidol University.

Figure 1. Strategy devised for the discovery of novel inhibitors. Pharmacophore searches based on the enzyme-inhibitor complexes of potent antifolates generated a focused database for docking.

unrelated to antifolates but inhibited the wild-type and mutant PfDHFRs in the micromolar range. The approach undertaken has proven to be effective for the discovery of new classes of inhibitors against malarial DHFR.

Results and Discussion

A focused strategy for "ad hoc" inhibitor discovery was devised and applied to PfDHFR. The strategy involved prefiltering the commercially available ACD database to select for molecules that match specific 3D-pharmacophore criteria suggested by the analysis of the enzyme-inhibitor complexes. This process served three purposes: first, to exclude "a priori" molecules that lack the chemical features crucial for interacting with key active site residues; second, to exclude molecules potentially unable to bind to the resistant mutant PfDHFRs; and third, to reduce the number of molecules to be screened in the docking process. Figure 1 illustrates the general strategy devised for discovery of novel inhibitors targeted against PfDHFRs. Three dimensional 3D pharmacophores were built and used to screen the entire available ACD database. In this respect, while 3D pharmacophores made of specific chemical fragments recognized to be crucial for activity are appropriate for finding analogues with improved potency (e.g., in lead optimization), those made of generic functions such as hydrogen bond donors and acceptors, general hydro-

phobic groups or aromatic rings, and molecular volumes are more appropriate for designing novel bioactive scaffolds. The resulting structures, grouped in a "focused database", were docked into the PfDHFR enzyme structure. The 24 best-scoring compounds chosen as described below were selected for further characterization (i.e., prediction of pK_a, energy minimization with AM1) and testing for their ability to inhibit the PfDHFR activity. Refinement of the ternary complexes with molecular mechanics and molecular dynamics simulations with the inclusion of solvent effects was subsequently performed for the active derivatives.

Figure 2 illustrates two examples of pharmacophores built upon protonated and neutral Cyc using Catalyst 4.6.[17] As previously reported for the model structure of the PfDHFR−NADPH−Cyc complex,[6] protonated Cyc forms bidentate hydrogen bonds with the carboxylate side chain of D54 via the N1-protonated nitrogen and the N6 amino groups (Figure 2A). These hydrogen bonds are conserved in several other antifolates whose crystal structures with DHFRs of different sources have been solved.[18−25] Indeed, interaction with the aspartic/glutamic acid corresponding to D54 in PfDHFR is known to be crucial for enzyme catalysis and inhibition of DHFRs,[26−28] and an increase in the apparent pK_a values for Pyr, MTX, and TMP upon binding to DHFRs has also been reported.[29,30] For these reasons, two hydrogen-bond donors corresponding to positions N1
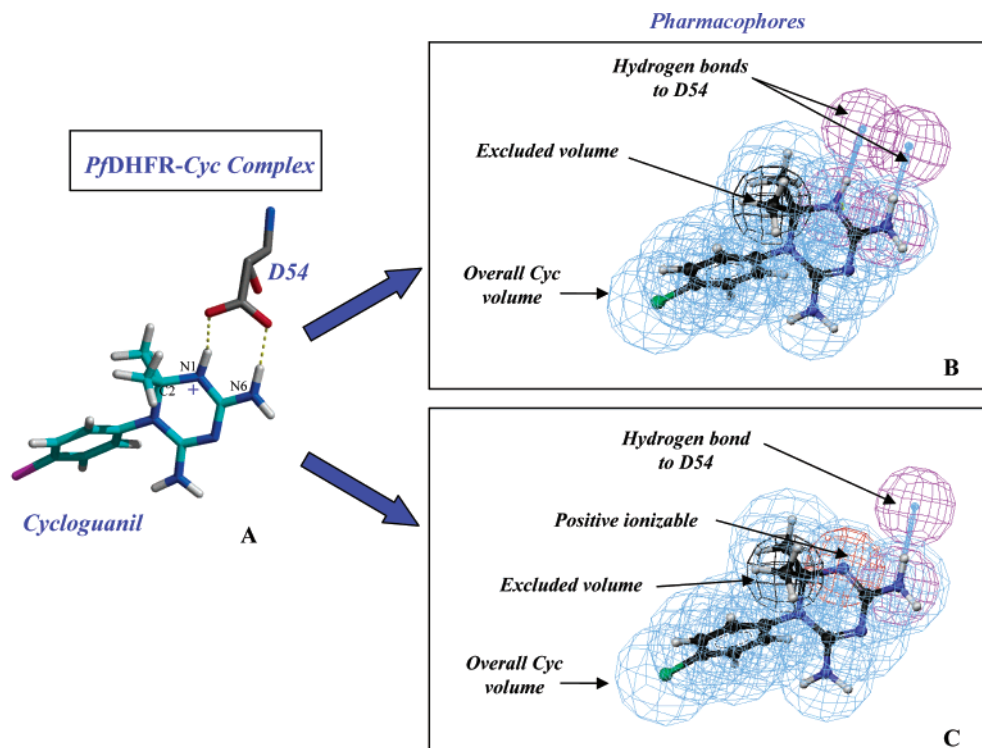
Figure 2. Two examples of pharmacophores built on the Cyc template: (A) structure of protonated form of Cyc showing bidentate hydrogen bonds with D54 of the PfDHFR−Cyc complex; (B) pharmacophore built on protonated Cyc showing two hydrogen bond donor vectors toward D54, the overall volume, and the excluded volume to avoid resistance; (C) pharmacophore built on neutral Cyc showing one hydrogen bond vector toward D54, one positive-ionizable group, the overall volume, and the excluded volume.

and N6 of protonated Cyc were built into the 3D pharmacophores (Figure 2B). In addition, the molecular volume of the inhibitor, in its enzyme-bound conformation, was included in the pharmacophores to filter for molecules that sterically complement the enzyme binding site. Likewise, pharmacophores that match the neutral Cyc, consisting of one hydrogen bond donor mapped on N6 and one positive-ionizable group mapped on N1, were also built and are shown in Figure 2C. These last pharmacophores allowed Catalyst to retrieve those compounds that do not have a hydrogen bond donor at N1 in their neutral forms but that could be converted to hydrogen bond donors after protonation of a nitrogen atom. The positive-ionizable function in Catalyst matches chemical fragments such as basic amines, amidines, guanidines, and positive charges. Since the presence of these fragments does not guarantee the protonation of these molecules at physiological pH, an estimate of the pK_a of the compounds in the hit list was made using the ACD/pKa software.[31] One important aspect of the Cyc-based pharmacophores was that the volume of one of the two methyl substituents at the C2 position of Cyc was excluded from the overall volume (parts B and C of Figure 2) to avoid steric clash with the A16V mutation in the Cyc-resistant PfDHFR.[6] This would permit retrieval of molecules that do not have any substituent in the sterically hindered and potentially resistant region of the active site.

Similarly to Cyc, pharmacophores were also generated using Pyr and WR99210 as templates. Since the A16V mutation does not confer resistance to these latter antifolates,[4,6] the excluded volume was not added. These resulted in a total of six pharmacophores that were used to screen the ACD, using the "fast−flexible" routine implemented in Catalyst. Once duplicates were re-

moved, the two pharmacophore searches based on Cyc, Pyr, and W99210 templates yielded a total of 594, 2183, and 2094 molecules, respectively. The relatively lower number of molecules retrieved with the Cyc pharmacophores compared to those with Pyr and WR99210 could be due to the excluded volume imposed in the former. The three databases were finally grouped into a single database that consisted of 4061 compounds after removal of duplications.

Scheme 1 shows the chemical families that emerge from the ACD screening using the pharmacophores. As requested, all the compounds possess either two hydrogen bond donors positioned to interact with D54 or one hydrogen bond donor and one nitrogen atom potentially able to protonate. They belong to several and diverse chemical families. The most well represented include hydrazines, ureas, thioureas, (thio)semicarbazides, (thio)-semicarbazones, guanides, biguanides, guanidines, amidines, and N-hydroxyamidines (Scheme 1), many of which have nitrogen- or oxygen-containing heterocycles (five- or six-membered or condensed rings) substituted with amino or hydroxyl groups. The screening also resulted in a huge number of primary, secondary, or tertiary diamines and hydroxyalkylamines, including some ammonium salts, and in a significant number of polyhydroxylated compounds such as pyranosides and furanosides. Owing to the molecular volume filter in the pharmacophores, the molecular weights of the resulting molecules were not higher than 400, thus meeting one of the conditions for druglike properties of a compound.[32]

Despite a drastic reduction of the number of compounds from the original 230 000 compounds in the ACD to the 4061 compounds in our focused database, there still remain a large number of significantly different chemical fragments that match the pharma-

Scheme 1. Chemical Families Emerging from the Pharmacophore Screening of the ACD[a]
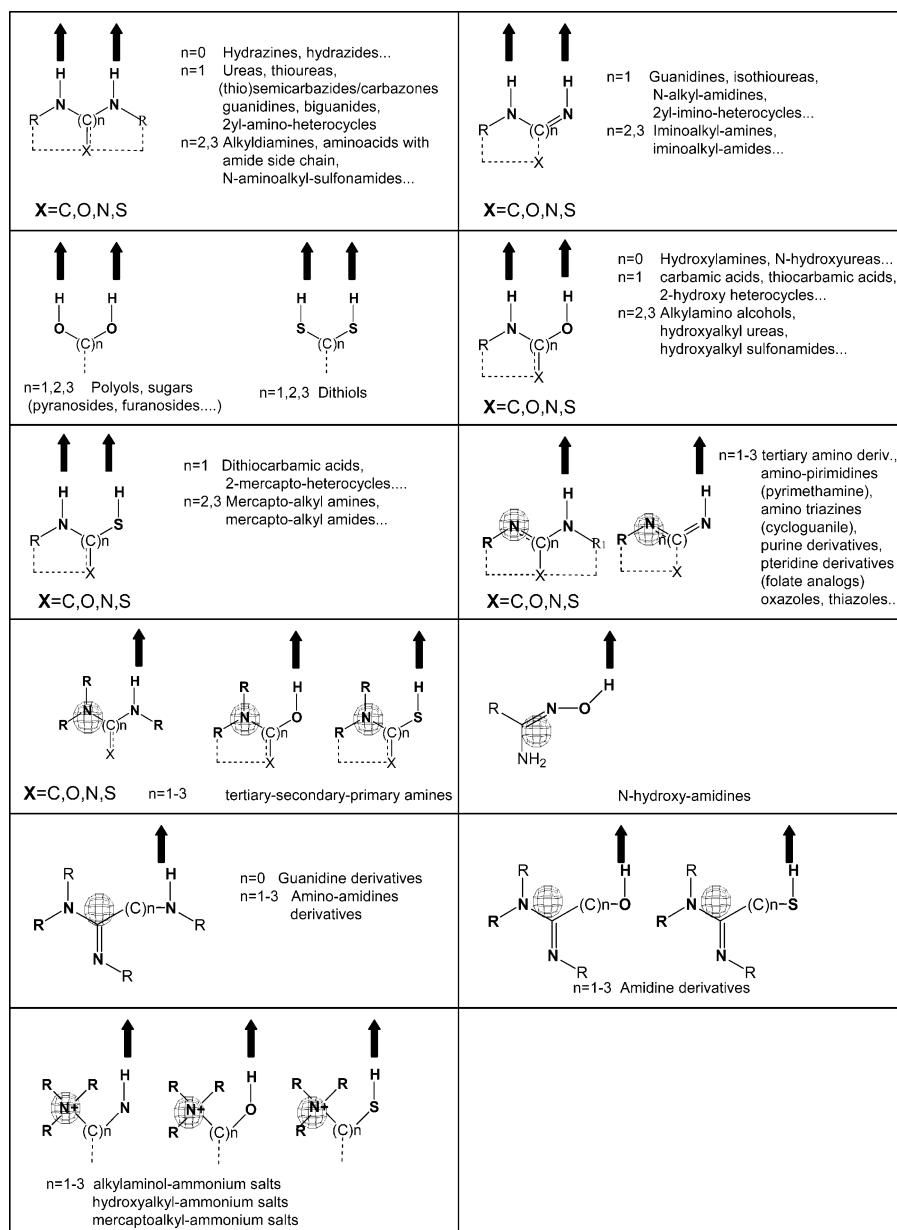
[a] Arrows correspond to hydrogen bond donors, and spheres correspond to positive-ionizable groups.

cophore requirements in the D54 region of the active site (Scheme 1). Further, the structures in other regions are highly varied because other features, except for the molecular volume, were not requested in the pharmacophores. The diversity of the focused database versus the entire ACD was quantitatively estimated by calculation of self-similarity for both databases using Tanimoto coefficients,[33] which are defined as $N_{AB}/(N_A + N_B - N_{AB})$, where N_A and N_B are the number of bit sets on (i.e., 1) in bit strings (binary representation of molecular structure) A and B, respectively, and N_{AB} is the number of bits that are in common. The value of the Tanimoto coefficient varies between 0 and 1. The lower the coefficient, the lesser is the similarity between the molecules being compared. The clustering of the molecules in the two databases was evaluated at fixed intervals of Tanimoto coefficients, and the results are graphically reported in Figure 3. While the trend observed for the entire ACD is very similar to that previously reported by Voigt et al,[34] the number of

clusters/entry of our focused database is always higher than that of the ACD (Figure 3), suggesting a better molecular diversity in the focused database. Our analyses are in line with a previous report[35] that demonstrated that docking molecules by chemical families increases the diversity of hits in database screening. Noteworthy is that while in that report the ACD was clustered into families sharing common but generic rigid fragments, our strategy was to cluster "families" of compounds based on specific 3D-pharmacophore requirements as guided by the enzyme-inhibitor complexes. To the best of our knowledge, this is a novel and more focused strategy that opens the way to increasing the chance of finding novel bioactive scaffolds.

Docking of the focused ACD database into the enzyme was then performed as described in the Experimental Section, using DOCK3.5.[36] The success of the docking approach depends heavily on the correctness of the PfDHFR homology model used. Evidence to support that this is indeed the case include the following. First, the
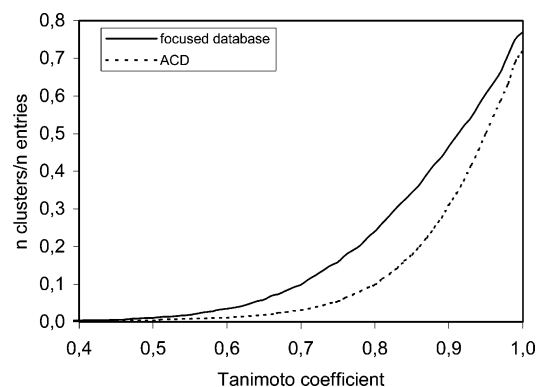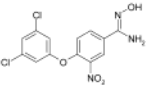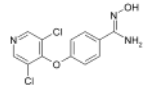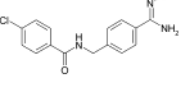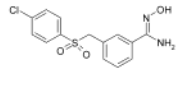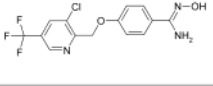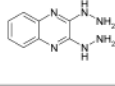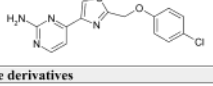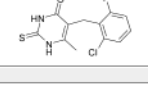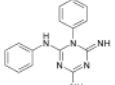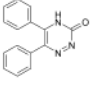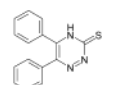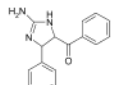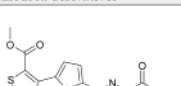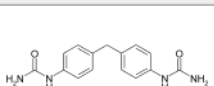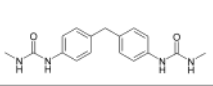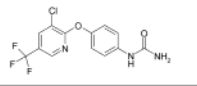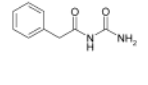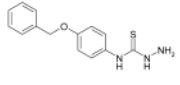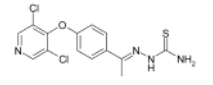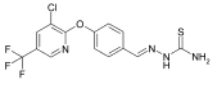
Figure 3. Molecular diversities of the focused (solid line) versus the entire ACD (dashed line) databases according to Tanimoto coefficent analysis. The number of clusters divided by the number of database entries are plotted against the Tanimoto coefficient values.

active site of most DHFRs is highly conserved, and hence, the architecture of the enzyme binding site in the PfDHFR homology model is very similar to that obtained from crystallographic studies.[6] Second, the homology model was previously tested experimentally with the structure-based design of inhibitors, and the results were as predicted.[6,9] Third, the inhibitor templates (Pyr, Cyc, and WR99210) were docked into the model of PfDHFR, and in all cases, the highest-score orientations found by docking (with scores of −49, −46, and −51 kcal/mol for Pyr, Cyc, and WR99210, respectively) were in full agreement with the orientations previously obtained from molecular mechanics and dynamics refinement of the complexes.[6] Fourth, we found here that several guanidine and folate analogues whose structures were closely related to classical antifolates including Pyr, Cyc, chlorguanide, and methotrexate were present as high-scoring compounds, suggesting that the approach is sensible for discovery of new chemical families as potential inhibitors of PfDHFRs.

The structures of the molecules that exhibited the best energy scores were visualized using MidasPlus and clustered into chemical families depending on the functional group interacting with D54. Before restriction of the selection of the compounds to the actual number of candidates here tested, the first 500 best-scoring compounds identified by DOCK, with docking scores between −52 and −20 kcal/mol, were visualized and analyzed. Among the chemical families that had the highest scores, we found *N*-hydroxyamidine, hydrazine, pyrimidine, triazine, dihydroimidazole, urea, and thiourea derivatives. Molecules related to classical antifolates, though present in the hit list, were not considered as candidates for biological testing. The analysis of the complexes also showed a number of recurrent features: compounds with the highest scores possessed functional groups able to hydrogen-bond to D54, I14, and/or I164, hydrophobic aromatic fragments close to the nicotinamide ring of NADPH, and in many cases a second hydrophobic aromatic fragment oriented toward the opening of the active site pocket and interacting mainly with I112 and P113.
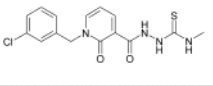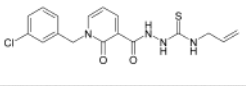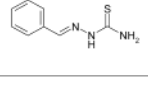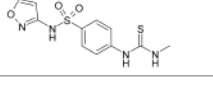
Although the docking scores, which are simply the sum of electrostatic and van der Waals interaction energies between enzyme and ligand, are known to correlate poorly with inhibitory activity,[37−39] they are

Table 1. Structures and Docking Scores of the Top-Scoring Compounds Selected from Docking of the Focused Database

a Docking scores (kcal/mol).

straightforward indices of complementarity for a database search. Therefore, the best-scoring compounds within each family were selected and analyzed for inhibitory activity against recombinant PfDHFR. A total of 24 compounds were obtained (Table 1), many of which were *N*-hydroxyamidines and (thio)ureas. These two classes in fact highly populated the hit list, and most of them had high scores. Since the docking procedure used is rigid (i.e., it does not take into account the conformational changes of enzyme and bound ligands), the structures of the selected PfDHFR inhibitor complexes

Table 2. Inhibition Constants (K_i, μM) of the Inhibitors against the Wild-Type PfDHFR and PfDHFRs with Single (A16V, S108T), Double (A16V + S108T), Triple (C59R + S108N + I164L), and Quadruple (N51I + C59R + S108N + I164L) Mutations

	P. falciparum DHFRs K_i (μM)					
compd	wild-type	A16V	S108T	A16V + S108T	C59R + S108N + I164L	N51I + C59R + S108N + I164L
Pyr[a]	0.0015 ± 0.0002	0.006 ± 0.001	0.0014 ± 0.0002	0.0036 ± 0.0003	0.38 ± 0.03	0.86 ± 0.12
Cyc[a]	0.0026 ± 0.0003	0.57 ± 0.04	0.0016 ± 0.0002	2.13 ± 0.10	1.14 ± 0.10	0.73 ± 0.02
1a	2.4 ± 0.2	36.8 ± 7.7	4.2 ± 0.5	9.8 ± 1.3	22.2 ± 5.2	32.6 ± 6.0
1b	25.2 ± 2.0	23.6 ± 2.5	16 ± 1.2	6.2 ± 0.6	24.4 ± 1.7	27.8 ± 1.7
1c	77.2 ± 13	58 ± 7	12.3 ± 1.1	57 ± 3.6	93 ± 5.3	36.6 ± 2.0
1d	102 ± 10	38 ± 2.4	30 ± 2.0	106 ± 4.8	105 ± 5.3	34.5 ± 2.4
2a	3.6 ± 1.1	3.4 ± 0.7	0.8 ± 0.1	11.4 ± 1.7	2.7 ± 0.6	9.7 ± 1.2
6a	9.7 ± 0.7	15.3 ± 1.1	4.2 ± 0.3	19.7 ± 1.2	7.5 ± 0.4	16.0 ± 1.0
6f	13.7 ± 1.7	15.4 ± 1.0	5.2 ± 0.8	55.6 ± 3.5	13.4 ± 0.9	26.5 ± 1.3
6g	0.9 ± 0.08	0.7 ± 0.1	1.0 ± 0.08	2.1 ± 0.2	0.6 ± 0.1	1.50 ± 0.03
6h	5.2 ± 0.8	6.8 ± 0.6	2.3 ± 0.2	34 ± 1.6	12.5 ± 1.1	9.3 ± 0.9
6i	11.3 ± 0.7	5.9 ± 0.6	1.8 ± 0.3	13.6 ± 2.9	7.1 ± 1.6	19.4 ± 2.3
6l	15.2 ± 0.7	13 ± 0.7	1.7 ± 0.2	17 ± 1.0	10 ± 0.6	10.6 ± 0.9
6m	23.6 ± 3.6	29.6 ± 6.4	9 ± 1.2	50.0 ± 8.2	28.9 ± 4.4	37.2 ± 4.6

[a] Data from ref 4.

were optimized using molecular mechanics and molecular dynamics simulations in water at 300 K (AMBER 6[40]). This approach proved to be successful in predicting the structures of novel inhibitors of aldose reductase.[41]

The structures of the selected compounds (Table 1) are considerably diverse from classical antifolates as well as from two inhibitors previously disclosed using docking,[42] the latter compounds being still reminiscent of the structures of Cyc and Pyr. The compounds in Table 1 were tested against the recombinant wild-type and five antifolate-resistant PfDHFRs containing A16V, S108T, A16V + S108T, C59R + S108N + I164L, and N51I + C59R + S108N + I164L mutations. The inhibition constants (K_i) were determined and compared to those of Pyr and Cyc (Table 2). While all of these compounds were less effective against the wild-type PfDHFR than Pyr and Cyc (they were effective against the mutant enzymes tested), they proved to inhibit enzyme activity in the micromolar range and they were completely different from already known inhibitors. Given that the preliminary goal of a 3D search is the search for new bioactive scaffolds from which subsequent modifications are needed in order to develop more potent inhibitors, our results represent a challenging step toward discovery of novel chemicals that are potential leads for further development.

Compounds **1a**–**e** are *N*-hydroxyamidine derivatives. The pK_a predictions suggested that the dissociation of the *N*-hydroxyl group occurs at a pH greater than 10, while the protonation of the amidine occurs at a pH less than 1.5. Accordingly, the compounds are predicted to be neutral at physiological pH. While the derivative **1e** was poorly soluble, the other four compounds (**1a**–**d**) inhibited the wild-type PfDHFR with K_i values ranging from 2.4 to 102 μM (Table 2). It is noteworthy that most of these compounds were active against the resistant mutants, with K_i values that are either ∼4-fold lower or up to 10-fold higher than that of the wild-type enzyme. This is in contrast with Pyr and Cyc, which inhibited the mutant enzymes at >200- to 800-fold increased K_i values (Table 2).[4]

In the complex between the most active *N*-hydroxyamidine derivative **1a** and wild-type PfDHFR (Figure 4A), the *N*-hydroxyl hydrogen-bonds to D54 while the nitrogen atom hydrogen-bonds to D54 via a water molecule. The amino substituent hydrogen-bonds to the

backbone carbonyl of I14 and gives one intramolecular hydrogen bond with the *N*-hydroxyl group. Similarly to the chlorophenyl ring of Pyr and Cyc,[6] the nitrobenzene ring of **1a** gives favorable interactions with the nicotinamide ring of NADPH while the 3,5-dichlorophenoxy ring extends toward the opening of the active site, adopting an orientation similar to that of the trichlorophenoxy ring of WR99210.[6] Compounds **1b**–**d** proved to be less active than **1a**, even though they retained activity for the resistant mutants. Given that all these derivatives display hydrogen bonds to D54 and I14 very similar to those observed for **1a**, the decrease in activity is likely due to differences in substituents and/or length and flexibility of the aryl side chain. Compared to **1a**, the smallest decrease in activity was found for compound **1b** (K_i = 25.2 μM). Compounds **1c** and **1d**, which possess a spacer of three and two atoms between the two aromatic rings, are about 30 and 40 times less active than **1a** against the wild-type enzyme, respectively. They displayed a significantly different orientation of the flexible arylalkyl side chains into the active site compared to **1a**. While the 3,5-dichlorophenyl ring of **1a** can adopt an orientation very similar to that of WR99210,[6] the corresponding rings of **1c** and **1d** assumed a significantly different orientation (data not shown).

Compound **2a** is a hydrazine derivative that emerged from docking. The compound inhibited the wild-type PfDHFR with a K_i value of 3.6 μM and also inhibited the antifolate-resistant PfDHFRs with comparable K_i values. Nevertheless, the compound was about 3-fold less active against the A16V + S108T mutant enzyme (Table 2). Considering the structure of the complex with wild-type PfDHFR (Figure 4B), four hydrogen bonds were predicted; one hydrazine substituent hydrogen-bonds with D54 and with the carbonyl oxygen of the nicotinamide of NADPH, whereas the other hydrazine substituent hydrogen-bonds with the backbone carbonyls of I14 and I164. The quinazoline ring of **2a** is inserted between the nicotinamide ring and the phenyl ring of F58, contributing favorably to the stabilization of the enzyme-inhibitor complex. Given the absence of bulky groups close to the A16 and S108 side chains, steric hindrance with resistant enzymes harboring the A16V and S108T mutations is not conceivable. This is in agreement with the data in Table 2, which show that
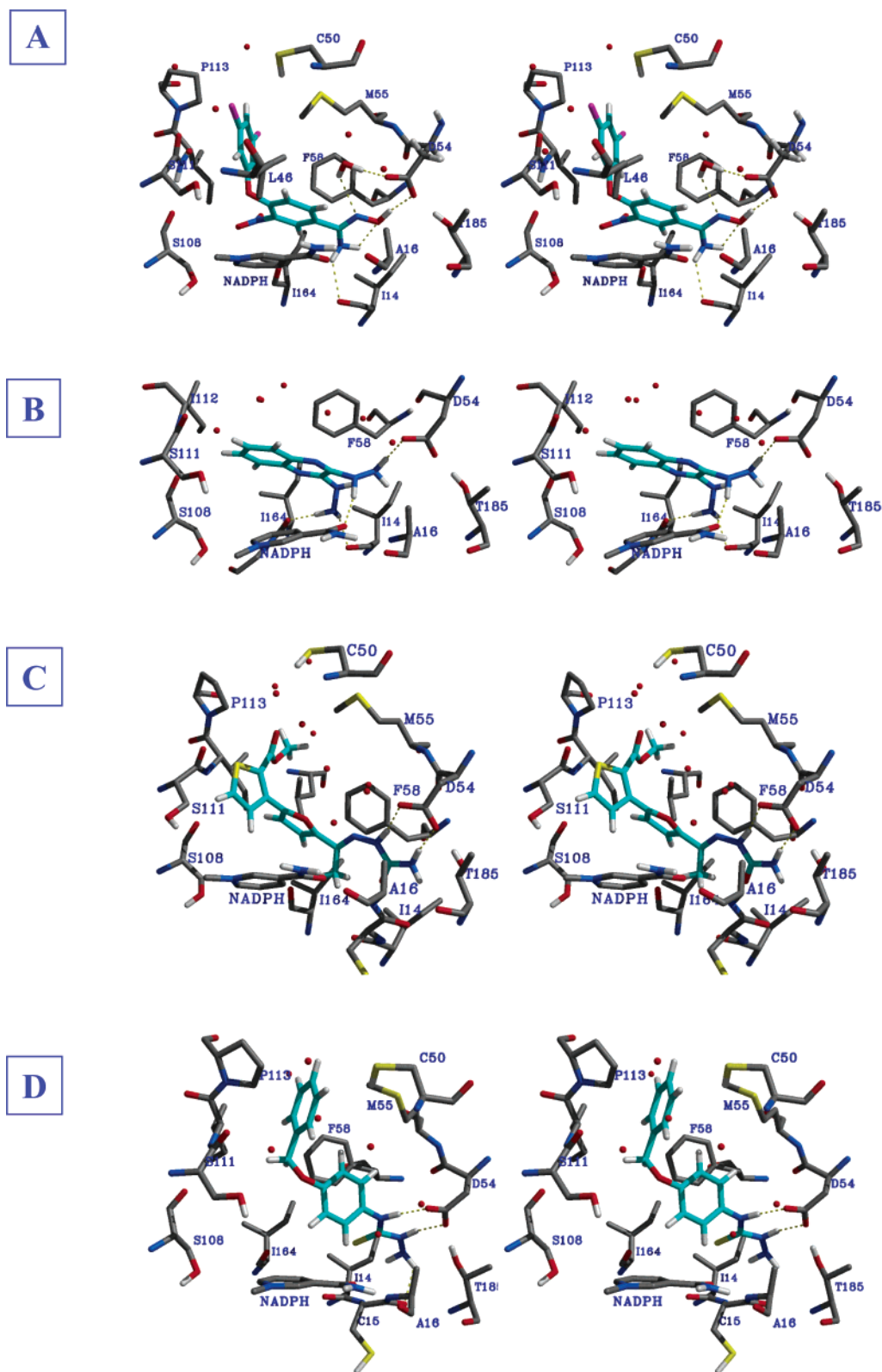
Figure 4. (Continued on next page)

2a binds the resistant PfDHFRs with similar affinity. Finally, given that the predicted pK_a value for compound **2a** is 4.2 and that there have been reports on the increase in the apparent pK_a values for Pyr, MTX, and TMP upon binding to DHFR,[29,30] it is anticipated that if compound **2a** indeed protonates, the protonated hydrazine would likely reinforce hydrogen bonds with the aspartate side chain of D54, contributing a salt link to the stabilization of the complex (Figure 4B). However, further experimental work is needed to obtain definitive conclusions.

The pyrimidine derivatives **3a** and **3b** (Table 1) were inactive against both wild-type and resistant mutant PfDHFRs. Compound **3a** was poorly soluble, with maximal solubility of about 25 μM. Compound **3b** was inactive up to a final concentration of 750 μM.
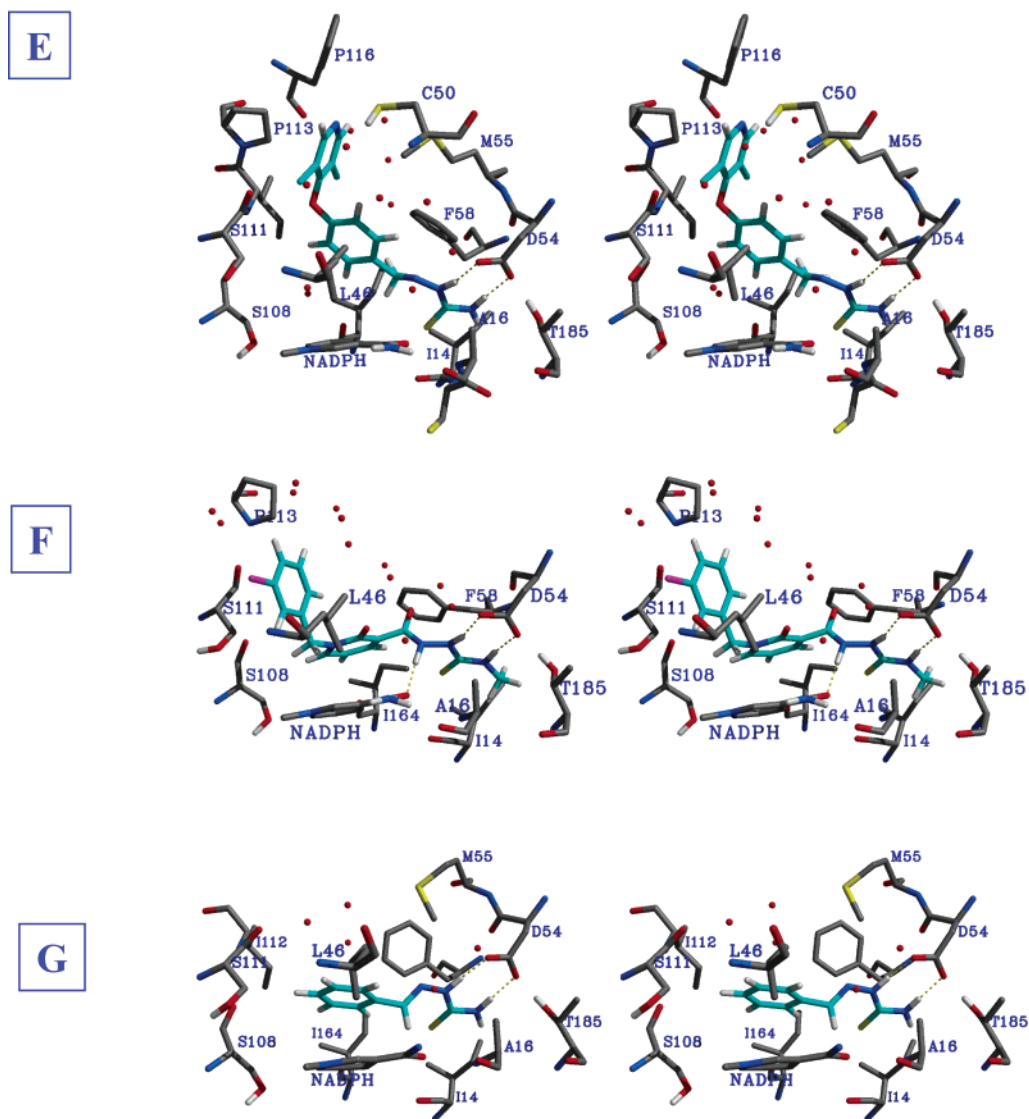
Figure 4. Stereoviews showing the active site residues of wild-type pfDHFR interacting with inhibitors **1a** (A), **2a** (B), **6a** (C), **6f** (D), **6g** (E), **6i** (F), and **6m** (G) after refinement of the complexes with MD. Only the polar hydrogens are shown. Hydrogen bonds are indicated as dotted lines, whereas water molecules are shown as red dots.

None of the triazine derivatives, compounds **4a**–**c** in Table 1, were active against the wild-type and resistant mutant pfDHFRs. Likewise, compound **5a**, a dihydroimidazole derivative, was inactive against all the enzymes tested up to a concentration of 100 μM.

Docking retrieved a considerable number of urea and thiourea derivatives as high-scoring compounds, some of which were selected and tested (compounds **6a**–**n** in Table 1). Among the urea derivatives (compounds **6a**–**e**) tested, only compound **6a** was active, while all the thiourea derivatives (compounds **6f**–**n**) except for **6n** were active against the wild-type and resistant enzymes. It is currently not clear why compound **6n** was inactive. However, the predicted dissociation of the sulfonamide nitrogen of **6n** at pH >5.0 might explain its ineffectiveness at physiological pH.

Compound **6a** inhibited the wild-type PfDHFR with a K_i value of 9.7 μM and the resistant PfDHFRs with similar inhibitory activities. As shown in Figure 4C, it forms a bidentate hydrogen bond to D54 via the urea nitrogens. The adjacent methyl group is close to the backbone carbonyls of I14 and I164, an orientation that is far from ideal. It is speculated that an amino

substituent in place of the methyl would lead to an increase of inhibitory activity because it would provide two additional hydrogen bonds with I14 and I164. The furyl ring is placed between the nicotinamide ring of NADPH and the phenyl ring of F58, and the thiophene substituent extends toward the opening of the active site and interacts mainly with the S111, P113, L46, and M55 side chains. Interestingly, these are the same residues that interact with the trichlorophenoxy ring of WR99210.[6]

The other urea derivatives, compounds **6b**–**e** in Table 1, are not active. Further, compounds **6b** and **6c** were poorly soluble. Comparison of the complexes of these inactive ureas with the complex of the active urea (**6a**) suggested that when the urea is directly attached to the aromatic ring, conformational constraints disfavor the concomitant formation of hydrogen bonds with D54 and aromatic–aromatic interactions with nicotinamide and F58.

The first compound in the thiourea series, **6f**, inhibited the wild-type PfHDFR with a K_i of 13.7 μM and the resistant mutants with similar K_i values. In the complex, compound **6f** forms a bidentate hydrogen bond to D54 via the thiourea nitrogens, while the extra amino

group interacts with the backbone carbonyl of C15 (Figure 4D). The phenyl ring interacts with the side chain of F58 while it is almost perpendicular to the nicotinamide ring of NADPH. The benzyloxy side chain is involved in hydrophobic interactions with residues P113, M55, and C50.

Compound **6g** inhibited wild-type PfDHFR with a K_i of 0.9 μM and was the most active inhibitor of both the wild-type and the resistant mutant PfDHFRs (Table 2). This compound forms a bidentate hydrogen bond to D54 via the thiourea nitrogens (Figure 4E). Unlike **6a**, the adjacent methyl group is still in proximity to I14 but significantly more distant from I164. The phenyl ring is close to the nicotinamide and F58, and the 3,5-dichloropyridinyl ring interacts with I112, P113, and M55.

Compound **6h** inhibited all PfDHFRs investigated but was about 5 times less active than **6g**. Compounds **6i** and **6l** inhibited the wild-type PfDHFR with K_i values of 11.3 and 15.2 μM, respectively, and were also active against the resistant mutant PfDHFRs (Table 2). As shown in Figure 4F, inhibitor **6i** adopted an orientation that is very similar to those previously described for other thioureas, with an additional hydrogen bond between the amide nitrogen and the carbonyl oxygen of the nicotinamide ring. Steric hindrance with A16V and S108T resistant mutants was not predicted, in agreement with experiment (Table 2). Compound **6l** binds very similarly to **6i**.

Compound **6m** is about 20 times less active than **6g**. It inhibited the wild-type PfDHFR with a K_i of 23.6 μM and also inhibited the antifolate-resistant mutants with similar K_i values (Table 2). While its binding orientation is similar to those described above, this compound is significantly shorter than other thioureas and interactions with P113, I112, and M55 cannot be formed.

Conclusions

We have presented a structure-based screening approach to search for novel classes of inhibitors of PfDHFR. In the search for molecules complementary with the enzyme active site, our strategy was to create a focused database of compounds that meet specific 3D-pharmacophore criteria based on important interactions with key amino acidic residues and to dock and score the resulting focused database in the putative pocket. This process served to exclude "a priori" molecules that lack the chemical features previously recognized to be crucial for the interaction with the enzyme, as well as molecules potentially unable to bind to resistant PfDH-FRs. We have shown that this new strategy significantly reduced the number of molecules required to be processed by docking and increased the chemical diversity of the database. Known antifolate inhibitors like Pyr, Cyc, chlorguanide, and methotrexate, as well as many and significantly diverse compounds, could be detected within the best-scoring list.

We have identified 12 new PfDHFR inhibitors whose structures are completely unrelated to those of the classical antifolates. Even if classical inhibitors such as Pyr and Cyc are considerably more active than the compounds disclosed in this study, the latter compounds are significantly diverse and inhibit PfDHFR in the micromolar range. Even more importantly, the inhibi-

tors presented in this study have the important advantage over Pyr and Cyc that they bind the resistant PfDHFRs with binding affinity similar to that observed for the wild-type enzyme, in agreement with the design. Further work will be needed to increase the potency of the new bioactive scaffolds here disclosed.

Experimental Section

Pharmacophore Screening of the ACD. A total of six 3D pharmacophores were constructed by assembling general chemical functions (hydrogen bond donors and positive-ionizable groups) and molecular volumes at the appropriate locations, using Catalyst 4.6.[17] These functions were mapped on the conformations of Pyr, Cyc, and WR99210 that bind pfDHFR.[6] In brief, all pharmacophores encode the possibilities of hydrogen-bonding to D54 (see Figure 2) either with two hydrogen bond donors mapped over the N1 and N6 atoms of protonated Pyr, Cyc, and WR99210 or with one positive-ionizable group mapped over the N1 nitrogen and one hydrogen bond donor mapped over the N6. This would permit retrieval of molecules that lack a hydrogen bond donor at N1 in the neutral form but that could be converted to a hydrogen bond donor after protonation. The hydrogen bond vectors and the positive-ionizable groups were restricted to appropriate positions using location constraints with tolerances of 1.5 Å. The final pharmacophores also included the overall volume of the templates (Pyr, Cyc, and WR99210) in order to remove from the list those compounds that have dimensions and shape significantly different from those of the active templates. The minimum similarity tolerance associated with these volumes, expressed as the volume of the intersection of two aligned molecules divided by the volume of their union, was set to 0.5. In the pharmacophores built on Cyc, an excluded volume corresponding to the C2 methyl group shown previously to be in steric conflict with the V16 side chain of the A16V resistant mutant[6] was added, which would permit retrieval of molecules that did not have any substituent in a sterically hindered and potentially resistant region of the active site. The radius of the excluded volume was set to 1.5 Å.

Once the six pharmacophores were built, each of them was used to screen the ACD database using the "fast–flexible" database search routine of Catalyst in which each compound had an associated conformational set within the 20 kcal/mol range of energy. The resulting compounds were grouped into a single focused database, and duplicates were removed.

Molecular Diversity Analysis. The diversity of the focused database and of the entire ACD was measured by means of a Tanimoto distance metric analysis.[33] Each database was first converted into smiles format, counterions were removed, and fingerprints were calculated using the 458 bit descriptors (E_SCREEN) implemented in the CACTVS system.[43] The Tanimoto analysis of the fingerprints was performed using SUBSET 1.0,[34,44] which estimates the molecular diversity of a database by a clustering approach. The number of clusters was calculated using Tanimoto coefficients ranging from 0 to 1, with 0.01 increments. Comparison of the diversity of the two different databases was achieved by dividing the number of clusters by the number of entries in each database.

Docking of the Focused Database. To prepare the focused database for DOCK3.5,[36] Sybyl atom types were automatically assigned using the sdf2mol2 utility. The Sybyl program was used to add hydrogens to the molecule, to assess the correct protonation state of charged functional groups such as carboxylates, guanidinium ions, etc., and to assign partial atomic charges according to Gasteiger–Marsili. The database was finally converted to a format recognizable by DOCK using the utility mol2db.

Docking was performed using the structure of the wild-type PfDHFR previously described.[6] The program SPHGEN[45] was used to generate clusters of overlapping spheres that describe the accessible surface of the active site. Sixty-six spheres were used to describe the active site. The module CHEMGRID[46] was used to precompute and save in a grid file the information

necessary for force field scoring. This scoring function approximates molecular mechanics interaction energies and consists of van der Waals and electrostatic components.[46]

DOCK3.5 was run to find and score orientations of each molecule of the databases into the active site of wild-type PfDHFR. Each orientation was filtered for steric fit with a DISTMAP grid[47] with polar and nonpolar contacts limits of 2.3 and 2.8 Å, respectively. Orientations that passed this steric filter were evaluated for van der Waals and electrostatic complementarity using the grids calculated by CHEMGRID.[46] The best-scoring compounds were saved and analyzed. Their complexes with PfDHFR were displayed with the computer graphics software Midas Plus.[48] The hit compounds were clustered into chemical families according to the functional group interacting with D54, and 24 candidates were finally selected.

Compounds Selected. Compounds were purchased from Sigma-Aldrich, Lancaster, Maybridge, Bionet, SPECS, and Transworld (Table 1). These include the following: (**1a**) 4-(3,5-dichlorophenoxy)-*N*-hydroxy-3-nitrobenzamidine; (**1b**) 4-(3,5-dichloropyridin-4-yloxy]-*N*-hydroxybenzamidine; (**1c**) 4-chloro-*N*-[4-(*N*-hydroxycarbamimidoyl)benzyl]benzamide; (**1d**) 3-(4-chlorobenzenesulfonylmethyl)-*N*-hydroxybenzamidine; (**1e**) 4-(3-chloro-5-trifluoromethylpyridin-2-ylmethoxy)-*N*-hydroxybenzamidine; (**2a**) rare chemicals RCL 2,894-1; (**3a**) 4-[2-(4-chlorophenoxymethyl)thiazol-4-yl]pyrimidin-2-ylamine; (**3b**) 5-(2-chloro-6-fluorobenzyl)-6-methyl-2-thioxo-2,3-dihydro-1*H*-pyrimidin-4-one; (**4a**) 6-imino-1,*N*2-diphenyl-1,6-dihydro-[1,3,5]-triazine-2,4-diamine; (**4b**) 5,6-diphenyl-4*H*-[1,2,4]triazin-3-one; (**4c**) 5,6-diphenyl-4*H*-[1,2,4]triazine-3-thione; (**5a**) (2-amino-5-phenyl-4,5-dihydro-3*H*-imidazol-4-yl)phenylmethanone; (**6a**) methyl 3-{5-[2-(aminomethyl)ethanhydrazonoyl]-2-furyl}thiophene-2-carboxylate; (**6b**) 4,4′-methylenebis(phenylurea); (**6c**) 4,4′-methylenebis(1-methyl-3-phenylurea); (**6d**) [4-(3-chloro-5-trifluoromethylpyridin-2-yloxy)phenyl]urea; (**6e**) phenylacetylurea; (**6f**) 4-(4-benzyloxyphenyl)-3-thiosemicarbazide; (**6g**) 2-(1-{4-[(3,5-dichloro-4-pyridyl)oxy]phenyl}ethylidene)hydrazine-1-carbothioamide; (**6h**) 4-[3-chloro-5-(trifluoromethyl)(2-pyridyl)oxy)]benzaldehydethiosemicarbazone; (**6i**) 1-(3-chlorobenzyl)-3-(1-(4-methylthiosemicarbazido)carbonyl)-2(1*H*)-pyridone; (**6l**) 1-(3-chlorobenzyl)-3-(1-(4-allylthiosemicarbazido)carbonyl)-2(1*H*)-pyridone; (**6m**) benzhaldehydethiosemicarbazone; (**6n**) *N*-(5-methylisoxazol-3-yl)-4-(3-methylthioureido)benzenesulfonamide.

Molecular Mechanics and Molecular Dynamics. The structures of the enzyme-inhibitor complexes were refined using a molecular mechanics force field and a molecular dynamics simulation protocol at 300 K. The sander_classic module of the AMBER 6[40] program and the Cornell et al.[49] force field were used.

To calculate partial atomic charges of inhibitors that were consistent with the AMBER force field, the geometries of the molecules were completely optimized using the AM1 Hamiltonian and charges were calculated with electrostatic potential fits to a 6-31G* ab initio wave function using Gaussian 98, followed by a standard RESP[50,51] fit. The van der Waals parameters of the inhibitors were assigned to be consistent with the Cornell force field, whereas the force field parameters for NADPH parameters were as previously described.[6]

Dihedral parameters consistent with the Cornell et al.[49] parametrization were assigned and, in some cases, were derived from a conformational analysis performed with AM1. Energy minimization with AMBER was performed to make sure that the optimized conformation was in agreement with the AM1-optimized conformation.

The effect of explicit water molecules in the enzyme-inhibitor complexes was included by solvating with spherical caps of TIP3P[52] water molecules within 31 Å of the inhibitors. On average, the number of water molecules was 2100, similar to our previous work.[6] Prior to energy minimization of the complexes, only the water molecules were energy-minimized and then subjected to 100 ps of molecular dynamics at 300 K to let the solvent equilibrate around the enzyme. Then 5000 steps of conjugate gradient energy minimization were per-

formed, and all protein residues within 10 Å from the inhibitor, the inhibitor, and all the water molecules were allowed to move. A 10 Å nonbonded cutoff was adopted in all simulations. Molecular dynamics of the PfDHFR-inhibitor complexes was then performed at 300 K for over 400 ps. The complexes were gradually heated to 300 K during the first 20 ps to avoid abrupt changes of structures. SHAKE[53] was turned on for bonds involving hydrogens, and a time step of 2 fs was used. During molecular dynamics, a 1 kcal/mol restraint on the backbone atoms of PfDHFR was applied, as from previous work,[6] to avoid undesirable drifts from experimentally validated structures of DHFRs. Coordinates during molecular dynamics were collected every 0.2 ps and averaged with CARNAL every 10 ps. Finally, the last 10 ps averaged structures were reoptimized with 5000 steps of conjugated gradient minimization.

Calculations were run on an IBM-SP3 computer at the Centro Interdipartimentale di Calcolo Elettronico ed Informatica Applicata of the University of Modena and Reggio Emilia. Graphic display and manipulation were performed on SGI O2 workstations.

Preparation of Recombinant PfDHFRs. The wild-type and mutants PfDHFRs were prepared following a previously reported procedure[4] in which the induction temperature was reduced to 20 °C and the induction time was prolonged to 20 h. The cell extract obtained after disruption of the bacterial cells by a French pressure cell at 18 000 psi was assayed for DHFR activities. The PfDHFRs were further purified by affinity chromatography using Methotrexate-Sepharose resin.[54]

Enzyme Assays and Inhibition. The activity of PfDHFR was determined spectrophotometrically according to the method previously described.[55] One unit of enzyme is defined as the amount of enzyme required to produce 1 μmol of product per min at 25 °C. The reaction mixture (1 mL) contained 1xDHFR buffer (50 mM TES, pH 7.0, 75 mM β-mercaptoethanol, 1 mg/mL bovine serum albumin), 100 μM each of the substrate H$_2$-folate and cofactor NADPH, and the appropriate amount (0.001−0.005 units) of the affinity-purified enzymes. For inhibition studies, the assay reaction mixture contained varying concentrations of inhibitor and all the ingredients except for enzyme and the reaction was initiated with purified recombinant enzyme (0.6−1 nM). All the inhibitors tested were dissolved in DMSO, of which the final concentration in the reaction was 1%. Depending on the solubility of the inhibitors, concentrations between 25 and 1000 μM were used. Assuming the inhibitors bind to the enzyme competitively, the K_i values of the inhibitors for the enzymes were determined by fitting to the equation IC$_{50}$ = $K_i(1 + ([S]/K_m))$,[56] where IC$_{50}$ is the concentration of inhibitor that inhibits 50% of the enzyme activity under standard assay conditions and K_m is the Michaelis constant for the substrate H$_2$-folate.

References

(1) Wirth, D. Malaria: a 21st century solution for an ancient disease. *Nat. Med.* **1998**, *4*, 1360−1362.
(2) Sirawaraporn, W. Dihydrofolate reductase and antifolate resistance in malaria. *Drug Resist. Updates* **1998**, *1*, 397−406.
(3) Warhurst, D. C. Resistance to antifolates in *Plasmodium falciparum*, the causative agent of tropical malaria. *Sci. Prog.* **2002**, *85*, 89−111.
(4) Sirawaraporn, W.; Sathitkul, T.; Sirawaraporn, R.; Yuthavong, Y.; Santi, D. V. Antifolate-resistant mutants of *Plasmodium falciparum* dihydrofolate reductase. *Proc. Natl. Acad. Sci. U.S.A.* **1997**, *94*, 1124−1129.
(5) Lemcke, T.; Christensen, I. T.; Jorgensen, F. S. Towards an understanding of drug resistance in malaria: three-dimensional structure of *Plasmodium falciparum* dihydrofolate reductase by homology building. *Bioorg. Med. Chem.* **1999**, *7*, 1003−1011.
(6) Rastelli, G.; Sirawaraporn, W.; Sompornpisut, P.; Vilaivan, T.; Kamchonwongpaisan, S.; Quarrell, R.; Lowe, G.; Thebtaranonth, Y.; Yuthavong, Y. Interaction of pyrimethamine, cycloguanil, WR99210 and their analogues with *Plasmodium falciparum* dihydrofolate reductase: structural basis of antifolate resistance. *Bioorg. Med. Chem.* **2000**, *8*, 1117−1128.

(7) Delfino, R. T.; Santos-Filho, O. A.; Figueroa-Villar, J. D. Molecular modeling of wild-type and antifolate resistant mutant *Plasmodium falciparum* DHFR. *Biophys. Chem.* **2002**, *98*, 287–300.

(8) Warhurst, D. C. Antimalarial drug discovery: development of inhibitors of dihydrofolate reductase active in drug resistance. *Drug Discovery Today* **1998**, *3*, 538–546.

(9) Yuthavong, Y.; Vilaivan, T.; Chareonsethakul, N.; Kamchonwongpaisan, S.; Sirawaraporn, W.; Quarrell, R.; Lowe, G. Development of a lead inhibitor for the A16V+S108T mutant of dihydrofolate reductase from the cycloguanil-resistant strain (T9/94) of *Plasmodium falciparum*. *J. Med. Chem.* **2000**, *43*, 2738–2744.

(10) Kuntz, I. D. Structure based strategies for drug design and discovery. *Science* **1992**, *257*, 1078–1082.

(11) Balbes, L. M.; Mascarella, S. W.; Boyd, D. B. A perspective of modern methods in computer-aided drug design. In *Reviews in Computational Chemistry*; Boyd, D. B., Ed.; VCH: New York, 1994; pp 337–379.

(12) Kuntz, I. D.; Meng, E. C.; Shoichet, B. K. Challenges in structure-based drug design. In *New Perspectives in Drug Design*; Newton, C. G., Ed.; Academic: London, 1995; pp 137–153.

(13) Mason, J. S.; McLay, I. M.; Lewis, R. A. Applications of computer-aided drug design techniques to lead generation. In *New Perspectives in Drug Design*; Newton, C. G., Ed.; Academic: London, 1995; pp 225–253.

(14) Shoichet, B. K.; Stroud, R. M.; Santi, D. V.; Kuntz, I. D.; Perry, K. M. Structure-based discovery of inhibitors of thymidylate synthase. *Science* **1993**, *259*, 1445–1450.

(15) Kuntz, I. D.; Meng, E. C.; Shoichet, B. K. Structure-based molecular design. *Acc. Chem. Res.* **1994**, *27*, 117–123.

(16) Good, A. C.; Mason, S. J. Three-dimensional structure database searches. In *Reviews in Computational Chemistry*; Boyd, D. B., Ed.; VCH: New York, 1996; pp 67–110.

(17) *Catalyst*, version 4.6; Accelrys: San Diego, CA, 2000.

(18) Volz, K. W.; Matthews, D. A.; Alden, R. A.; Freer, S. T.; Hansch, C.; Kaufman, B. T.; Kraut, J. Crystal structure of avian dihydrofolate reductase containing phenyltriazine and NADPH. *J. Biol. Chem.* **1982**, *257*, 2528–2536.

(19) Oefner, C.; D'Arcy, A.; Winkler, F. K. Crystal structure of human dihydrofolate reductase complexed with folate. *Eur. J. Biochem.* **1988**, *174*, 377–385.

(20) Bystroff, C.; Oatley, S. J.; Kraut, J. Crystal structures of *Escherichia coli* dihydrofolate reductase: the NADP$^+$ holoenzyme and the folate NADP$^+$ ternary complex. Substrate binding and a model for the transition state. *Biochemistry* **1990**, *29*, 3263–3277.

(21) Davies, J. F.; Delcamp, T. J.; Prendergast, N. J.; Ashford, V. A.; Freisheim, J. H.; Kraut, J. Crystal structures of recombinant human dihydrofolate reductase complexed with folate and 5-deazafolate. *Biochemistry* **1990**, *29*, 9467–9479.

(22) McTigue, M. A.; Davies, J. F., 2nd; Kaufman, B. T.; Kraut, J. Crystal structure of chicken liver dihydrofolate reductase complexed with NADP+ and biopterin. *Biochemistry* **1992**, *31*, 7264–7273.

(23) McTigue, M. A.; Davies, J. F.; Kaufman, B. T.; Kraut, J. Crystal structures of chicken liver dihydrofolate reductase: binary thioNADP$^+$ and ternary thioNADP$^+$·biopterin complexes. *Biochemistry* **1993**, *32*, 6855–6862.

(24) Reyes, V. M.; Sawaya, M. R.; Brown, K. A.; Kraut, J. Isomorphous crystal structures of *Escherichia coli* dihydrofolate reductase complexed with folate, 5-deazafolate, and 5,10-dideazatetrahydrofolate: mechanistic implications. *Biochemistry* **1995**, *34*, 2710–2723.

(25) Cody, V.; Galitsky, N.; Luft, J. R.; Pangborn, W.; Blakley, R. L.; Gangjee, A. Comparison of ternary crystal complexes of F31 variants of human dihydrofolate reductase with NADPH and a classical antitumor furopyrimidine. *Anti-Cancer Drug Des.* **1998**, *13*, 307–315.

(26) Howell, E. E.; Villafranca, J. E.; Warren, M. S.; Oatley, S. J.; Kraut, J. Functional role of aspartic acid-27 in dihydrofolate reductase revealed by mutagenesis. *Science* **1986**, *231*, 1123–1128.

(27) David, C. L.; Howell, E. E.; Farnum, M. F.; Villafranca, J. E.; Oatley, S. J.; Kraut, J. Structure and function of alternative proton-relay mutants of dihydrofolate reductase. *Biochemistry* **1992**, *31*, 9813–9822.

(28) Sirawaraporn, W.; Sirawaraporn, R.; Yongkiettrakul, S.; Anuwatwora, A.; Rastelli, G.; Kamchonwongpaisan, S.; Yuthavong, Y. Mutational analysis of *Plasmodium falciparum* dihydrofolate reductase: the role of aspartate 54 and phenylalanine 223 on catalytic activity and antifolate binding. *Mol. Biochem. Parasitol.* **2002**, *121*, 185–193.

(29) Cocco, L.; Groff, J. P.; Temple, C., Jr.; Montgomery, J. A.; London, R. E.; Blakley, R. L. Carbon-13 nuclear magnetic resonance study of protonation of methotrexate and aminopterin bound to dihydrofolate reductase. *Biochemistry* **1981**, *20*, 3972–3978.

(30) Cocco, L.; Roth, B.; Temple, C., Jr.; Montgomery, J. A.; London, R. E.; Matwiyoff, N. A. Protonated state of methotrexate, trimethoprim, and pyrimethamine bound to dihydrofolate reductase. *Arch. Biochem. Biophys.* **1983**, *226*, 567–577.

(31) *ACD/log D Suite*, version 4.5; Advanced Chemistry Development: Toronto, Canada.

(32) Lipinski, C. A. Drug-like properties and the causes of poor solubility and poor permeability. *J. Pharmacol. Toxicol. Methods* **2000**, *44*, 235–249.

(33) Dean, P. M., Ed. *Molecular similarity in drug design*; Blackie Academic & Professional: London, 1995; pp 111–137.

(34) Voigt, J. H.; Bienfait, B.; Wang, S.; Nicklaus, M. C. Comparison of the NCI open database with seven large chemical structural databases. *J. Chem. Inf. Comput. Sci.* **2001**, *41*, 702–712.

(35) Su, A. I.; Lorber, D. M.; Weston, G. S.; Baase, W. A.; Matthews, B. W.; Shoichet, B. K. Docking molecules by families to increase the diversity of hits in database screens: computational strategy and experimental evaluation. *Proteins* **2001**, *42*, 279–293.

(36) Gschwend, D. A.; Kuntz, I. D. Orientational sampling and rigid-body minimization in molecular docking revisited: on-the-fly optimization and degeneracy removal. *J. Comput.-Aided Mol. Des.* **1996**, *10*, 123–132.

(37) Bohm, H. J. Prediction of binding constants of protein ligands: a fast method for the prioritization of hits obtained from de novo design or 3D database search programs. *J. Comput.-Aided Mol. Des.* **1998**, *12*, 309–323.

(38) Muegge, I.; Martin, Y. C. A general and fast scoring function for protein–ligand interactions: a simplified potential approach. *J. Med. Chem.* **1999**, *42*, 791–804.

(39) Tame, J. R. Scoring functions: a view from the bench. *J. Comput.-Aided Mol. Des.* **1999**, *13*, 99–108.

(40) Case, D. A.; Pearlman, D. A.; Caldwell, J. W.; Cheatman, I.; Ross, W. S.; Simmerling, C. L.; Darden, T. A.; Merz, K. M.; Stanton, R. V.; Cheng, A. L.; Vincent, J. J.; Crowley, M.; Tsui, V.; Radmer, R. J.; Duan, Y.; Pitera, J.; Massova, I.; Seibel, G. L.; Singh, U. C.; Weiner, P. K.; Kollman, P. A. *AMBER*, version 6.0; University of California, San Francisco, CA, 1999.

(41) Rastelli, G.; Ferrari, A. M.; Costantino, L.; Gamberini, M. C. Discovery of new inhibitors of aldose reductase from molecular docking and database screening. *Bioorg. Med. Chem.* **2002**, *10*, 1437–1450.

(42) Toyoda, T.; Brobey, R. K.; Sano, G.; Horii, T.; Tomioka, N.; Itai, A. Lead discovery of inhibitors of the dihydrofolate reductase domain of *Plasmodium falciparum* dihydrofolate reductase–thymidylate synthase. *Biochem. Biophys. Res. Commun.* **1997**, *235*, 515–519.

(43) Ihlenfeldt, W. D.; Takahashi, Y.; Abe, S.; Sasaki, S. Computation and management of chemical properties in CACTVS: an extensible networked approach toward modularity and compatibility. *J. Chem. Inf. Comput. Sci.* **1994**, *34*, 109–116.

(44) SUBSET is available at http://cactus.nci.nih.gov/SUBSET/.

(45) Kuntz, I. D.; Blaney, J. M.; Oatley, S. J.; Langridge, R.; Ferrin, T. E. A geometric approach to macromolecule–ligand interactions. *J. Mol. Biol.* **1982**, *161*, 269–288.

(46) Meng, E. C.; Shoichet, B. K.; Kuntz, I. D. Automated docking with grid based energy evaluation. *J. Comput. Chem.* **1992**, *13*, 505–524.

(47) Shoichet, B. K.; Bodian, D. L.; Kuntz, I. D. Molecular docking using shape descriptors. *J. Comput. Chem.* **1992**, *13*, 380–397.

(48) Ferrin, T. E.; Huang, C. C.; Jarvis, L. E.; Langridge, R. The MIDAS display system. *J. Mol. Graphics* **1988**, *6*, 13–27.

(49) Cornell, W. D.; Cieplak, P.; Bayly, C. I.; Gould, I. R.; Merz, K. M., Jr.; Ferguson, D. M.; Spellmeyer, D. C.; Fox, T.; Caldwell, J. W.; Kollman, P. A. A second generation force field for the simulation of proteins, nucleic acids, and organic molecules *J. Am. Chem. Soc.* **1995**, *117*, 5179–5197.

(50) Bayly, C. I.; Cieplak, P.; Cornell, W. D.; Kollman, P. A. A well behaved electrostatic potential based method using charge restraint for deriving atomic charges: the RESP model. *J. Phys. Chem.* **1993**, *97*, 10269–10283.

(51) Cieplak, P.; Bayly, C. I.; Cornell, W. D.; Kollman, P. A. Application of the multimolecule and multiconformational RESP methodology to biopolymers charge derivation for DNA, RNA and proteins. *J. Comput. Chem.* **1995**, *16*, 1357–1377.

(52) Jorgensen, W. L.; Chandrasekhar, J.; Madura, J. D.; Impey, R. W.; Klein, M. L. Comparison of simple potential functions for simulating liquid water. *J. Chem. Phys.* **1983**, *79*, 926–935.

(53) Van Gusteren, W. F.; Berendsen, H. J. C. Algorithms for macromolecular dynamics and constraint dynamics. *Mol. Phys.* **1977**, *34*, 1311–1327.

(54) Meek, T. D.; Garvey, E. P.; Santi, D. V. Purification and characterization of the bifunctional thymidylate synthetase–dihydrofolate reductase from methotrexate resistant *Leishmania tropica*. *Biochemistry* **1985**, *24*, 678–686.

(55) Sirawaraporn, W.; Prapunwattana, P.; Sirawaraporn, R.; Yuthavong, Y.; Santi, D. V. The dihydrofolate reductase domain of *Plasmodium falciparum* thymidylate synthase–dihydrofolate reductase: gene synthesis, expression, and anti-folate resistant mutants. *J. Biol. Chem.* **1993**, *268*, 21637–21644.

(56) Segal, I. H. Behavior and analysis of steady-state and rapid equilibrium enzyme systems. In *Enzyme Kinetics*; Segal, I. H., Ed.; Wiley-Interscience: New York, 1975; pp 100–160.